

A Quasi-Random Approach to Space-Time Codes ¹

Keying Wu¹, Li Ping¹ and Jinhong Yuan²

¹City University of Hong Kong, Hong Kong and ²University of New South Wales, Australia

Abstract

This paper presents a quasi-random approach to space-time (ST) codes. The basic principle is conceptually simple, yet still very effective and flexible regarding the transmission rate and antenna numbers. We outline a turbo-type iterative decoding algorithm with complexity growing linearly with the transmit antenna number, and independently of the layer number. We develop simple techniques for fast performance assessment. Based on these techniques, efficient power allocation strategies are examined, which greatly enhance the system performance. Simulation results show that the proposed code can achieve near-capacity performance at low decoding complexity.

1. Introduction

The spatial diversity provided by multiple-input-multiple-output (MIMO) systems can be used to significantly increase the reliability and spectrum efficiency of wireless communication systems [1]. Various transmission schemes have been developed to efficiently exploit such spatial diversity [2]-[6]. Although great achievement has been made, there are still many open problems. Most good ST codes are designed for specific numbers of transmit antennas, and a unified approach is lacking for systems with arbitrary numbers of transmit antennas. It is also difficult to achieve performance close to the theoretical limits [1] of high-rate multiple transmit antenna systems.

This paper is concerned with a quasi-random approach to ST coding, referred to as the interleave-division-multiplexing space-time (IDM-ST) scheme. The basic idea is very simple: we employ several forward error correction (FEC) codes, and transmit their randomly interleaved codewords simultaneously from all antennas. This scheme is applicable to arbitrary numbers of transmit antennas.

Random interleaving is a key operation here and provides the only means to separate signals from different antennas and layers. The motivation is random coding. We will show that the random coding approach can be applied to developing ST codes. Specifically,

- We describe encoding methods to construct ST codes that resemble random ST codes with i.i.d. Gaussian elements.
- We outline a low-cost iterative decoding procedure with complexity (per coded bit) that grows only linearly with the number of transmit antennas.
- For performance assessment, we develop a signal-to-noise-ratio (SNR) evolution technique for fixed channels and a bounding technique for quasi-static fading channels. These techniques are simple, fast and relatively accurate.

Using the fast performance assessment techniques, we examine efficient power allocation strategies to maximize

energy efficiency gain. The proposed scheme can achieve performance close to the theoretical limit.

2. Transmitter Principles

2.1. Motivations

The motivation of this work comes from the concept of “random coding”, which is an optimal scheme from information theory point of view. Consider a one-dimensional (1D) conventional code represented by a length- I sequence,

$$s_1, s_2, \dots, s_i, s_{i+1}, \dots, s_{I-1}, s_I$$

and a two-dimensional (2D) ST code represented by a $N \times J$ matrix,

$$\begin{matrix} s_1^{(1)} & \cdots & s_J^{(1)} \\ \vdots & \ddots & \vdots \\ s_1^{(N)} & \cdots & s_J^{(N)} \end{matrix}$$

where N is the number of transmit antennas, I and J are both code lengths. A code (either 1D or 2D) is said to be “random” if its elements are independent and identically distributed (i.i.d.). In many applications, the Gaussian distribution is optimal for mutual information maximization. Clearly, a $N \times J$ 2D random code can be generated by segmenting a length- $(N \times J)$ 1D random code into N rows, which suggests a simple way to form a 2D random code from a 1D random code. This is the rationale behind the scheme presented below. Our task is to make the resultant code practical, in particular easy to encode and decode.

2.2. Transmitter Structures

The interleave-division-multiplexing space-time (IDM-ST) coding scheme is developed based on the above discussion. We first consider the encoder structure shown in Fig. 1(a).

Superposition encoder in Fig. 1(a): The inputs are K equal-length sequences $\{d_k\}$, each encoded individually using a binary FEC code, generating c_k . The signals from the same encoder are referred to as a layer. For simplicity, we use the

¹ This work was fully supported by a grant from the Research Grant Council of the Hong Kong SAR, China [CityU 1314/04E].

same FEC code C for all layers. Each \mathbf{c}_k is segmented into N sections in the serial-to-parallel (S/P) converter, which are then independently interleaved, QPSK modulated, scaled by a common amplitude factor $\sqrt{p_k}$, and transmitted from N antennas in parallel. On each antenna, signals from K layers are linearly superimposed and transmitted simultaneously. Denote by R_C the rate of C . The overall rate $R = 2NKR_C$, where the factor “2” comes from the QPSK modulation.

Suppose that C is an ideal “random” binary code over $\{+1, -1\}$. From the Central Limit Theorem, after QPSK modulation and the summation in Fig. 1(a), the elements transmitted from different antennas are approximately i.i.d. circularly symmetric complex Gaussian random variables for a sufficiently large K . Thus Fig. 1(a) is an approximate realization of the scheme discussed in Section 2.1.

It is reasonable to expect that “nearly random” binary codes, such as turbo and LDPC codes, may also be used for C in this scheme. The use of interleavers and power controllers in Fig. 1(a) is to facilitate the iterative detection process, which will be discussed in detail in Sections 3 and 5.

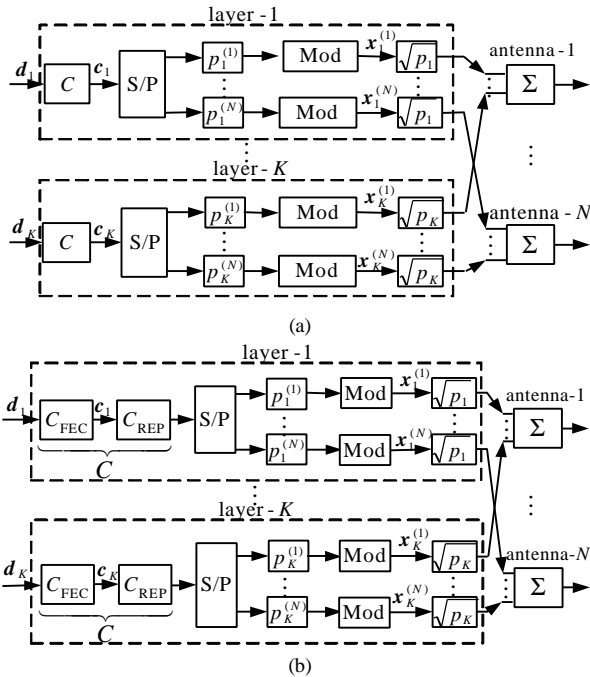


Figure 1. (a) Transmitter structure of a superposition IDM-ST code, where $p_k^{(n)}$ is the interleaver for layer- k on antenna- n , “Mod” denotes a QPSK modulator, and “S/P” denotes a serial-to-parallel converter. (b) Transmitter structure of a repetition-superposition IDM-ST code, where C_{FEC} denotes a binary FEC code and C_{REP} a length- N repetition code.

Repetition-superposition encoder in Fig. 1(b): Consider a special case of Fig. 1(a). Assume that (i) C is constructed by serially concatenating a binary FEC code and a length- N repetition code; and (ii) the S/P converters are designed such that N replicas of each FEC coded bit are transmitted from N different antennas. These two constraints introduce symmetry in the proposed scheme and simplify the analysis and design issues (see Section 4). Fig. 1(b) shows the resultant transmitter structure. Each data sequence \mathbf{d}_k is first

encoded by a binary FEC code C_{FEC} , generating $\mathbf{c}_k = \{c_{k,i}\}$ ($c_{k,i} \in \{+1, -1\}$). Each \mathbf{c}_k is repeated N times and segmented in a S/P converter into N equal-length sections. The S/P converters are designed such that each section is a replica of the corresponding \mathbf{c}_k . The n th replica of \mathbf{c}_k is independently interleaved and QPSK modulated, producing $\mathbf{x}_k^{(n)} \equiv \{x_{k,j}^{(n)}\}$ to be transmitted from the n th antenna. (Here we always assume Gray mapping.) The interleavers for different layers and replicas are generated independently and randomly. Signals in $\{\mathbf{x}_k^{(n)}, n=1 \sim N\}$ are scaled by a common amplitude factor $\sqrt{p_k}$. For the n th transmit antenna, the transmitted signal is $\sum_{k=1}^K \sqrt{p_k} \mathbf{x}_k^{(n)}$. Denote by R_C the rate of C_{FEC} . Then $R = 2KR_C$.

Although the repetition operation above implies sub-optimality in terms of coding gain, later we will show in Section 6 that this scheme can still achieve relatively good performance.

The concept of “layer” here is different from that in the BLAST scheme [4]. Each layer in the IDM-ST scheme is transmitted from all antennas simultaneously and therefore there is interference among the signals in the same layer. There is no limit on the number of layers in the IDM-ST scheme. On the other hand, in the BLAST scheme, there is no interference among signals in the same layer, and the number of layers is limited by the number of antennas.

In the following, we first discuss the repetition-superposition IDM-ST transmitter structure in Fig. 1(b), since it is easier to analyze and design. Later, in Section 6, we will demonstrate the advantage of removing repetition coding.

3. Receiver Principles

We concentrate on MISO systems with N transmit antennas and one receive antenna (a $N \times 1$ system) over flat quasi-static Rayleigh fading channels. Let $\mathbf{a}^{(n)}$ ($n = 1, \dots, N$) be the fading coefficient between the n th transmit antenna and the receive antenna. $\{\mathbf{a}^{(n)}\}$ are modeled as independent complex Gaussian random variables with zero-mean and variance $\sigma^2 = 0.5$ per dimension. We always assume no channel state information (CSI) at the transmitter and ideal CSI at the receiver.

Consider the transmitter structure in Fig. 1(b). The signal received at time j is

$$y_j = \sum_{n=1}^N \mathbf{a}^{(n)} \sum_{k=1}^K \sqrt{p_k} x_{k,j}^{(n)} + n_j = \mathbf{a}^{(n)} \sqrt{p_k} x_{k,j}^{(n)} + \mathbf{z}_{k,j}^{(n)} \quad (1a)$$

where

$$\mathbf{z}_{k,j}^{(n)} = \sum_{(n',k') \neq (n,k)} \mathbf{a}^{(n')} \sqrt{p_{k'}} x_{k',j}^{(n')} + n_j \quad (1b)$$

and $\{n_j\}$ are samples of a complex additive white Gaussian noise (AWGN) process with variance $\sigma^2 = N_0/2$ per dimension. We employ a sub-optimal iterative receiver, which consists of an Elementary Signal Estimator (ESE) module and K a posteriori probability (APP) decoders

(DECs) operating iteratively [7]. Fig. 2 illustrates a part of the receiver structure in which only the DEC for layer- k (denoted by DEC- k) is shown. The DECs for other layers are connected to the ESE in the same way as DEC- k .

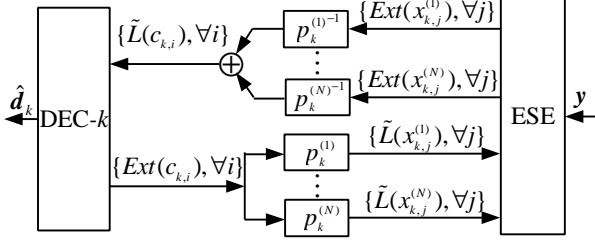


Figure 2. A part of the receiver structure of the IDM-ST code in Fig. 1(b) related to layer- k , where $\mathbf{y} = \{y_j\}$. The DECs for other layers are connected to the ESE in the same way as DEC- k .

For simplicity, we first assume BPSK modulation, i.e., $x_{k,j}^{(n)} = \pm 1$. We introduce the following definitions for a complex variable a :

$$E(a) \equiv E(\text{Re}(a)) + iE(\text{Im}(a)), \quad (2a)$$

and

$$\text{Cov}(a) \equiv \begin{pmatrix} \text{Var}(\text{Re}(a)) & \text{Cov}(\text{Re}(a), \text{Im}(a)) \\ \text{Cov}(\text{Re}(a), \text{Im}(a)) & \text{Var}(\text{Im}(a)) \end{pmatrix}, \quad (2b)$$

where

$$\text{Cov}(b, c) = E(b \cdot c) - E(b)E(c).$$

We also define

$$\mathbf{R}^{(n)} \equiv \begin{pmatrix} \text{Re}(\mathbf{a}^{(n)}) & -\text{Im}(\mathbf{a}^{(n)}) \\ \text{Im}(\mathbf{a}^{(n)}) & \text{Re}(\mathbf{a}^{(n)}) \end{pmatrix}, \quad (3)$$

The main decoding operations for BPSK modulation are listed below. (For the detailed derivation, please refer to [7].

We will denote by $\overline{\mathbf{a}^{(n)}}$ the conjugate of $\mathbf{a}^{(n)}$ in the following.)

(a) Initialization: Set $\tilde{L}(x_{k,j}^{(n)}) = 0 \quad \forall n, j$.

(b) Main iteration:

$$E(x_{k,j}^{(n)}) = \tanh(\tilde{L}(x_{k,j}^{(n)})/2). \quad (4a)$$

$$\text{Var}(x_{k,j}^{(n)}) = 1 - (E(x_{k,j}^{(n)}))^2. \quad (4b)$$

$$E(y_j) = \sum_{k,n} \mathbf{a}^{(n)} \sqrt{p_k} E(x_{k,j}^{(n)}). \quad (5a)$$

$$\text{Cov}(y_j) = \sum_{n,k} p_k \mathbf{R}^{(n)} \text{Cov}(x_{k,j}^{(n)}) (\mathbf{R}^{(n)})^T + \mathbf{s}^2 \mathbf{I}. \quad (5b)$$

$$E(\overline{\mathbf{a}^{(n)}} \mathbf{z}_{k,j}^{(n)}) = \overline{\mathbf{a}^{(n)}} (E(y_j) - \mathbf{a}^{(n)} \sqrt{p_k} E(x_{k,j}^{(n)})). \quad (6a)$$

$$\text{Cov}(\overline{\mathbf{a}^{(n)}} \mathbf{z}_{k,j}^{(n)}) = (\mathbf{R}^{(n)})^T (\text{Cov}(y_j) - p_k \mathbf{R}^{(n)} \text{Cov}(x_{k,j}^{(n)}) (\mathbf{R}^{(n)})^T) \mathbf{R}^{(n)}. \quad (6b)$$

$$\text{Ext}(x_{k,j}^{(n)}) = 2 |\mathbf{a}^{(n)}|^2 \sqrt{p_k} \cdot \frac{\text{Re}(\overline{\mathbf{a}^{(n)}} y_j) - E(\text{Re}(\overline{\mathbf{a}^{(n)}} \mathbf{z}_{k,j}^{(n)}))}{\text{Var}(\text{Re}(\overline{\mathbf{a}^{(n)}} \mathbf{z}_{k,j}^{(n)}))}. \quad (7)$$

$$\tilde{L}(c_{k,i}) = \sum_{(n,j) \in S(c_{k,i})} \text{Ext}(x_{k,j}^{(n)}). \quad (8)$$

In (8), $S(c_{k,i})$ is the index set of the N replicas related to $c_{k,i}$ in $\{x_{k,j}^{(n)}, \forall n, j\}$ (for all (n, j) combinations). Each DEC- k

carries out APP decoding at this stage using $\{\tilde{L}(c_{k,i}), \forall i\}$ as the input to produce extrinsic LLRs $\{\text{Ext}(c_{k,i}), \forall i\}$ for c_k , which are then used to update $\{\tilde{L}(x_{k,j}^{(n)}), \forall n, j\}$ as (assuming $(n, j) \in S(c_{k,i})$)

$$\tilde{L}(x_{k,j}^{(n)}) = \text{Ext}(c_{k,i}). \quad (9)$$

Then go back to (4) for the next iteration. After the final iteration, the DEC makes a hard decision $\hat{\mathbf{d}}$ on \mathbf{d} .

Instead of (9), we can also adopt the following updating rule.

$$\tilde{L}(x_{k,j}^{(n)}) = \text{Ext}(c_{k,i}) + \sum_{\substack{(n',j') \in S(c_{k,i}) \\ (n',j') \neq (n,j)}} \text{Ext}(x_{k,j'}^{(n')}). \quad (10)$$

The LLRs in the last term in (10) represent independent information (assuming sufficiently long random interleavers) with respect to observation y_j . We have found that using (10) in simulation leads to better performance than using (9). However, it is easier to develop analysis and optimization techniques based on (9), as will be explained in Section 4.

With QPSK modulation, $x_{k,j}^{(n)} = \text{Re}(x_{k,j}^{(n)}) + i \text{Im}(x_{k,j}^{(n)})$ with $\text{Re}(x_{k,j}^{(n)})$ and $\text{Im}(x_{k,j}^{(n)})$ two coded bits from c_k . Similar to (7), we have,

$$\text{Ext}(\text{Re}(x_{k,j}^{(n)})) = 2 |\mathbf{a}^{(n)}|^2 \sqrt{p_k} \cdot \frac{\text{Re}(\overline{\mathbf{a}^{(n)}} y_j) - E(\text{Re}(\overline{\mathbf{a}^{(n)}} \mathbf{z}_{k,j}^{(n)}))}{\text{Var}(\text{Re}(\overline{\mathbf{a}^{(n)}} \mathbf{z}_{k,j}^{(n)}))}. \quad (11)$$

The estimate of $\text{Im}(x_{k,j}^{(n)})$, denoted by $\text{Ext}(\text{Im}(x_{k,j}^{(n)}))$, can be calculated similarly to (11), with “Re” replaced by “Im”. Consequently, the estimate of each $c_{k,i}$ is calculated as

$$\tilde{L}(c_{k,i}) = \sum_{(n,j) \in S_R(c_{k,i})} \text{Ext}(\text{Re}(x_{k,j}^{(n)})) + \sum_{(n,j) \in S_I(c_{k,i})} \text{Ext}(\text{Im}(x_{k,j}^{(n)})), \quad (12)$$

where $S_R(c_{k,i})$ and $S_I(c_{k,i})$ are the index sets of the N replicas of $c_{k,i}$ in $\{\text{Re}(x_{k,j}^{(n)}), \forall n, j\}$ and $\{\text{Im}(x_{k,j}^{(n)}), \forall n, j\}$ respectively. Eqns. (9) and (10) should be modified accordingly.

4. Performance Analysis

The performance assessment of ST codes is generally a difficult issue, which involves integration over multi-dimensional distributions of the fading coefficients on all antennas, and can be difficult to implement. It turns out that a simple solution exists for IDM-ST codes. Due to the random interleaving used, the IDM-ST code possesses similar randomness to turbo and LDPC codes. This randomness property allows the use of analytical tools such as the EXIT chart and density evolution methods [8], where performance evaluation is carried out based on the average mutual information or SNR measures.

In the following, we introduce an evaluation method for the IDM-ST code. The method is semi-analytical since some functions (related to the FEC codes) are pre-calculated by simulation (similarly to [9]). The basic principle is similar to the EXIT chart. It is simple, fast and relatively accurate.

4.1. Performance Analysis with Fixed Fading Coefficients

All discussions in this section are for QPSK modulation. We first consider fixed fading coefficients $\mathbf{a} \equiv [\mathbf{a}^{(1)} \cdots \mathbf{a}^{(N)}]$. Substituting (1a) into (11), we can calculate the SNR for $Ext(\text{Re}(x_{k,j}^{(n)}))$ with respect to $\text{Re}(x_{k,j}^{(n)})$, denoted by $snr_{\text{Re},k,j}^{(n)}$, as (Please refer to [7] for the detailed derivation.)

$$snr_{\text{Re},k,j}^{(n)} = \frac{E(|\mathbf{a}^{(n)}|^2 \sqrt{p_k} \text{Re}(x_{k,j}^{(n)}))^2}{\text{Var}(\text{Re}(\mathbf{z}_{k,j}^{(n)}))} = \frac{|\mathbf{a}^{(n)}|^4 p_k}{\text{Var}(\text{Re}(\mathbf{z}_{k,j}^{(n)}))}. \quad (13)$$

The SNR for $Ext(\text{Im}(x_{k,j}^{(n)}))$ with respect to $\text{Im}(x_{k,j}^{(n)})$ can be calculated similarly to (13) with “Re” replaced by “Im”. Substituting (1a) and (11) into (12), we can see that $\tilde{L}(c_{k,i})$ is a maximum ratio combining (MRC) of N independently distorted signals in $S_R(c_{k,i})$ and $S_I(c_{k,i})$, apart from a scaling factor of 2. Thus, the SNR of $\tilde{L}(c_{k,i})$, denoted by $snr_{k,i}$, is given by [10]

$$snr_{k,i} = \sum_{(n,j) \in S_R(c_{k,i})} \frac{|\mathbf{a}^{(n)}|^4 p_k}{\text{Var}(\text{Re}(\mathbf{z}_{k,j}^{(n)}))} + \sum_{(n,j) \in S_I(c_{k,i})} \frac{|\mathbf{a}^{(n)}|^4 p_k}{\text{Var}(\text{Im}(\mathbf{z}_{k,j}^{(n)}))}. \quad (14)$$

Averaging $snr_{k,i}$ over all i , we define

$$\begin{aligned} snr_k &\equiv E(sn_{k,i}) \\ &= E\left(\sum_{(n,j) \in S_R(c_{k,i})} \frac{|\mathbf{a}^{(n)}|^4 p_k}{\text{Var}(\text{Re}(\mathbf{z}_{k,j}^{(n)}))} + \sum_{(n,j) \in S_I(c_{k,i})} \frac{|\mathbf{a}^{(n)}|^4 p_k}{\text{Var}(\text{Im}(\mathbf{z}_{k,j}^{(n)}))} \right) \\ &\stackrel{(a)}{\geq} \sum_{(n,j) \in S_R(c_{k,i})} \frac{|\mathbf{a}^{(n)}|^4 p_k}{E(\text{Var}(\text{Re}(\mathbf{z}_{k,j}^{(n)})))} + \sum_{(n,j) \in S_I(c_{k,i})} \frac{|\mathbf{a}^{(n)}|^4 p_k}{E(\text{Var}(\text{Im}(\mathbf{z}_{k,j}^{(n)})))} \\ &\stackrel{(b)}{=} \sum_{n=1}^N \frac{|\mathbf{a}^{(n)}|^2 p_k}{\sum_{(k',n) \neq (k,n)} |\mathbf{a}^{(n')}|^2 p_{k'} v_{k'} + \mathbf{s}^2}, \end{aligned} \quad (15)$$

$$\text{where } v_k \equiv E(\text{Var}(c_{k,i})) \quad (16)$$

is the average variance of $\{c_{k,i}, \forall i\}$ calculated based on the output of DEC- k [7]. In (15), (a) follows from Jensen’s inequality [11] since $snr_{k,i}$ is a convex function of each

$\text{Var}(\text{Re}(\mathbf{z}_{k,j}^{(n)}))$ and $\text{Var}(\text{Im}(\mathbf{z}_{k,j}^{(n)}))$ involved, and (b) is derived in [7]. In (15), snr_k is not a function of i , but is still a function of k , since each layer k may have a different transmission power level p_k . We point out that the simple expression in (15) is the consequence of the symmetry introduced by the repetition operation in Fig. 1(b).

Define

$$\mathbf{g}_k \equiv \sum_{n=1}^N \frac{|\mathbf{a}^{(n)}|^2 p_k}{\sum_{(k',n) \neq (k,n)} |\mathbf{a}^{(n')}|^2 p_{k'} v_{k'} + \mathbf{s}^2}. \quad (17)$$

From (15), \mathbf{g}_k is a lower bound of snr_k . In the following, we use this lower bound to approximate snr_k , as it is easy to calculate. Since v_k is generated using the output of DEC- k , it is a function of the average input SNR to DEC- k , i.e.,

$$v_k = f(\mathbf{g}_k). \quad (18)$$

In general, there is no closed-form expression for $f(\cdot)$, but we can (approximately) obtain this Var-SNR transfer relationship using Monte Carlo simulation for C_{FEC} in an AWGN channel with specified SNRs. Similarly we can define the frame-error-rate performance for DEC- k , denoted by FER_k , as a function of \mathbf{g}_k , i.e.,

$$\text{FER}_k = g(\mathbf{g}_k) \quad (19)$$

which can also be obtained by Monte Carlo simulation. From (17) and (18), we have

$$\mathbf{g}_{k,\text{new}} = \sum_{n=1}^N \frac{|\mathbf{a}^{(n)}|^2 p_k}{\sum_{(k',n) \neq (k,n)} |\mathbf{a}^{(n')}|^2 p_{k'} f(\mathbf{g}_{k',\text{old}}) + \mathbf{s}^2} \quad (20)$$

where $\mathbf{g}_{k,\text{new}}$ and $\mathbf{g}_{k,\text{old}}$ (initialized to 1 for $\forall k$) are the values of \mathbf{g}_k after and before one iteration. Repeating (20), we can track the SNR evolution in the iterative process with any given \mathbf{a} . After the final iteration, we can estimate the frame-error-rate performance of layer- k using (19) as

$$\text{FER}_k = g(\mathbf{g}_{k,\text{final}}). \quad (21)$$

4.2. Performance Analysis in Quasi-Static Fading Channels

The above discussion is for fixed \mathbf{a} . We now consider a quasi-static Rayleigh fading channel where \mathbf{a} remains unchanged during one frame and varies independently from frame to frame. Considering all possible \mathbf{a} , the average frame-error-rate of layer- k can be estimated as

$$\text{FER}_{k,\text{fading}} = \int g(\mathbf{g}_{k,\text{final}}) p(\mathbf{a}) d\mathbf{a}, \quad (22)$$

where $p(\mathbf{a})$ is the joint pdf of $\{\mathbf{a}^{(1)}, \dots, \mathbf{a}^{(N)}\}$. The computation of (22) is relatively difficult since it involves an N -fold multiple integral. To avoid this difficulty, we introduce a bounding technique. Denote $\mathbf{I} \equiv \sum_n |\mathbf{a}^{(n)}|^2 = \mathbf{a} \mathbf{a}^H$. It can be shown that \mathbf{g}_k in (17) is lower-bounded as [7]

$$\mathbf{g}_k \geq \frac{\mathbf{I} p_k}{\mathbf{I} \sum_{k'} p_{k'} v_{k'} - \mathbf{I} p_k v_k / N + \mathbf{s}^2}, \quad (23)$$

where the equality holds when $|\mathbf{a}^{(1)}|^2 = \dots = |\mathbf{a}^{(N)}|^2 = \mathbf{I} / N$.

It can be verified that $g(\cdot)$ in (19) is a decreasing function, so $\text{FER}_{k,\text{fading}}$ in (22) can be upper bounded as

$$\text{FER}_{k,\text{fading}} \leq \int g(\bar{\mathbf{g}}_{k,\text{final}}) p(\mathbf{I}) d\mathbf{I}, \quad (24)$$

where $p(\mathbf{I}) = \mathbf{I}^{N-1} e^{-\mathbf{I}} / (N-1)!$ is the pdf of \mathbf{I} and $\bar{\mathbf{g}}_{k,\text{final}}$ is calculated using the following iteration

$$\bar{\mathbf{g}}_{k,\text{new}} = \frac{\mathbf{I} p_k}{\mathbf{I} \sum_{k'} p_{k'} f(\bar{\mathbf{g}}_{k',\text{old}}) - \mathbf{I} p_k f(\bar{\mathbf{g}}_{k,\text{old}}) / N + \mathbf{s}^2}, \quad (25)$$

with $f(\bar{\mathbf{g}}_{k,\text{old}})$ initialized to 1 for $\forall k$.

Compared with (22), the upper bound in (24) is much easier to calculate as it involves only a one-fold integral.

Several approximations are involved in the above bounding technique, so it is necessary to examine its usefulness. Fig. 3 compares the simulation and upper bound results for 2×1 and 4×1 IDM-ST codes based on Fig. 1(b) with $R = 4$ bits per channel use. The detailed parameters will be explained in Section 6. As we can see, the upper bound is relatively tight. It provides a fast and relatively accurate approach to performance assessment of the repetition-superposition IDM-ST code.

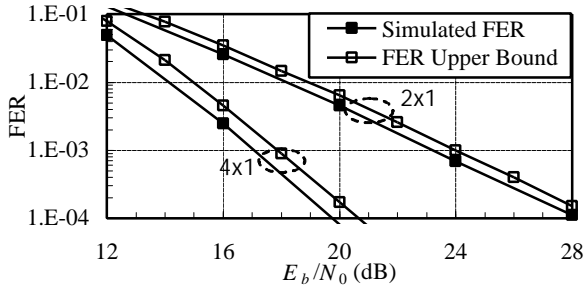


Figure 3. Comparison between the upper bound and simulation results for 2×1 and 4×1 IDM-ST codes based on Fig.1(b) with $R = 4$ bits per channel use.

4.3. Power Allocation

The SNR evolution techniques developed above can be used to optimize IDM-ST codes. It can be verified that, for any fixed \mathbf{a} and $P \equiv \sum_k p_k$, the outcome of (22) depends on the distribution of $\{p_1, \dots, p_K\}$. The aim of power allocation [12] is to search for a distribution of $\{p_k\}$ that optimizes the system performance for a fixed total power $P = \sum_k p_k$. The SNR evolution technique introduced above can be used for fast performance assessment in the search process. A detailed discussion of power allocation techniques can be found in [7][13].

5. Numerical Results

Let N_{info} be the number of information bits per layer in a frame, R the overall transmission rate, R_C the rate of C_{FEC} , and It the iteration number. We use (10) instead of (9) for all simulation results, since it leads to better performance. We call each \mathbf{d}_k a frame and $\{\mathbf{d}_k, k=1, \dots, K\}$ a super-frame. The frame error rate (FER) and super-frame error rate (SFER) are defined accordingly. Clearly, $\text{SFER} \geq \text{FER}$.

Consider 2×1 and 4×1 IDM-ST coding systems based on Fig. 1(b) with $N_{\text{info}} = 4096$, $It = 40$, $R = 4$ bits per channel use, corresponding to $K=6$. A rate-1/3 turbo code with generator $G(x)=(1+x+x^3)/(1+x^2+x^3)$ is used for all layers. The power levels for different layers are listed in Table 1. (Note: From simulation results, proper power allocation is necessary for the IDM-ST code to work with $R \geq 2$.) Fig. 4 shows the simulated performance of the above two IDM-ST systems over quasi-static Rayleigh fading channels. Corresponding outage probabilities [1] are included for reference, which serve as theoretical limits for SFER. From this figure, we can see that the FER behavior of the IDM-ST codes is quite close to the outage probabilities (within 1.5

dB). SFER is 0.5 ~ 1.5 dB worse than FER. However in practice, FER can be a more useful performance measurement than SFER, as in case of error it is only necessary to discard the erroneous frames, instead of the complete super-frame.

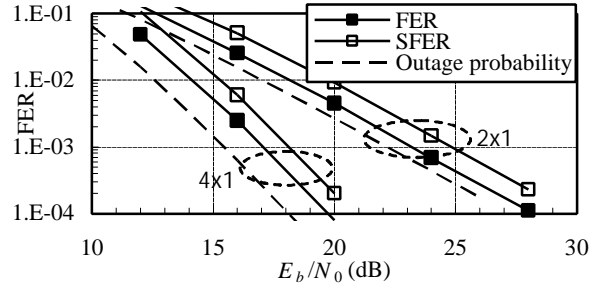


Figure 4. FER and SFER performance of 2×1 and 4×1 IDM-ST coding systems based on Fig. 1(b) with $R = 4$ bits per channel use over a quasi-static Rayleigh fading channel. $N_{\text{info}} = 4096$, $It = 40$.

Table 1. Power levels allocated to different layers for the IDM-ST coding systems in Fig. 4, where P is the total power of all layers.

(N, R, K)	Power Levels
(2, 4, 6)	0.0242P, 0.045P, 0.0806P, 0.1439P, 0.2543P, 0.452P
(4, 4, 6)	0.0268P, 0.0461P, 0.0809P, 0.1421P, 0.2521P, 0.452P

We now compare the two alternatives in Figs.1(a) and 1(b). The transmitter structure in Fig.1(a) allows the use of more sophisticated low-rate codes with higher coding gain. Fig. 5 compares the FER performance for these two alternatives with $N_{\text{info}} = 4096$, $It = 40$, $N = 4$, $R=2/3$ and 2 bits per channel use over quasi-static Rayleigh fading channels. The parameters for the FEC codes used in the two schemes are as follows.

The repetition-superposition IDM-ST code in Fig. 1(b)

(Scheme I): We employ the same rate-1/3 turbo code as that in Fig. 4. $K=1$ and 3 for $R=2/3$ and 2, respectively. The power levels for $K=3$ are 0.1737P, 0.2983P and 0.528P.

The superposition IDM-ST code in Fig. 1(a) (Scheme II):

We employ a turbo-Hadamard code [14] with $R_C= 1/12$, $M=3$, $r=4$, $G(x)=1/(1+x)$, where M is the number of component codes, r is the order of the Hadamard code used, and $G(x)$ is the generator of the convolutional code involved. $K=1$ and 3 for $R=2/3$ and 2, respectively. The power levels for $K=3$ are 0.18P, 0.2823P and 0.5377P.

From this figure we can see that the scheme in Fig. 1(a) can further improve the system performance, thanks to the additional coding gain provided by the better low-rate code. However, the use of non-repeated low-rate codes complicates the performance analysis issue (see Section 4.1), and makes power allocation a more difficult task. The power levels used in Fig. 5 are obtained from a simulation-based search. With a large number of layers, such a search method becomes too time-consuming. Efficient solutions to this problem are still under investigation.

Fig. 6 compares the IDM-ST codes with some existing ST codes, including the algebraic ST code [5], the serial

concatenated ST block code (STBC) [3] and trellis-coded modulation (TCM) code [15], and the ST trellis code [16]. All codes have $R=2$ bits per channel use. The IDM-ST codes use the same FEC code as in Fig. 4. The performance curves of other ST codes are cited from the corresponding references. As we can see, the IDM-ST code always has the superior performance, and the advantage grows with the number of transmit antennas.

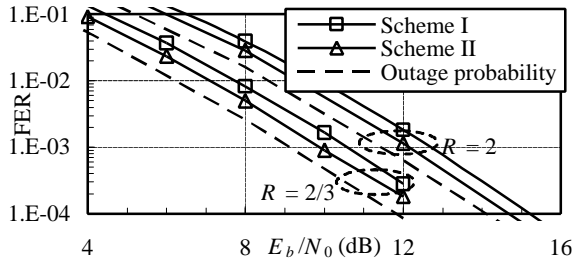


Figure 5. Performance comparison between the IDM-ST systems based on Figs. 1(a) and 1(b) over quasi-static Rayleigh fading channels with $N = 4$, $N_{info} = 4096$, $I_t = 40$, $R = 2/3$ and 2 bits per channel use.

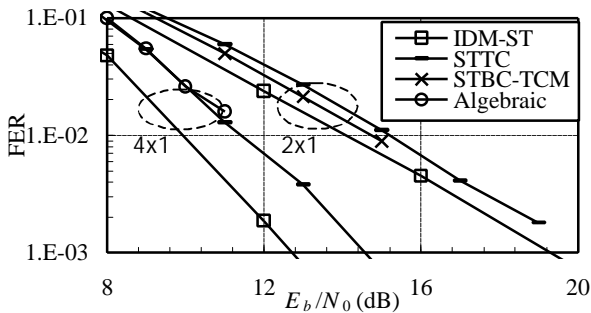


Figure 6. Comparison between the IDM-ST code and other ST codes.

6. Discussions and Conclusions

We have demonstrated a number of advantages of IDM-ST codes, including: simple design procedure, low receiver complexity, flexibility regarding the number of transmit antennas, and near-capacity performance at high rates. These advantages indicate good potentials of the proposed code for applications in various wireless environments.

The IDM-ST code provides a promising and unified solution to ST coding for high-rate application with arbitrary numbers of transmit antennas. It also has good potential for applications in ad hoc networks and relay channels. For example, consider a relay channel with a set of transmitting terminals. Each source terminal wants to transmit information to a single destination terminal, and potentially uses other terminals as relays [17], as shown in Fig. 7. Each relay may become active or inactive depending on the channel condition without informing the source terminal, so the number of active relays may not be fixed in advance. Suppose that we want to apply ST coding techniques in such a scenario to improve diversity gain [17]. Traditional ST transmission schemes will encounter difficulties in these applications since most of them are designed for specific transmit antenna numbers. For the IDM-ST code, however,

the number of transmit antennas can be set freely. This clearly indicates the advantages of the proposed IDM-ST code.

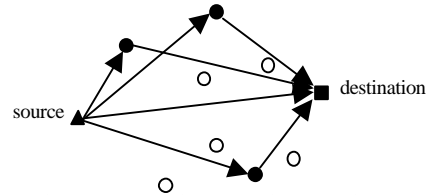


Figure 7. A relay channel model, where black circles denote active relays and white circles inactive relays.

REFERENCES

- [1] G. J. Foschini and M. Gans, "On the limits of wireless communication in a fading environment when using multiple antennas," *Wireless Personal Commun.*, vol. 6, pp. 311-335, Mar. 1998.
- [2] V. Tarokh, N. Seshadri, and A. R. Calderbank, "Space-time codes for high data rate wireless communication: performance analysis and code construction," *IEEE Trans. Inform. Theory*, vol. 44, pp. 744-765, Mar. 1998.
- [3] S. M. Alamouti, "A simple transmit diversity technique for wireless communications," *IEEE J. Select. Areas Commun.*, vol. 16, no. 8, pp. 1451-1458, Oct. 1998.
- [4] G. J. Foschini, "Layered space-time architecture for wireless communication in fading environment when using multiple antennas," *Bell Labs Tech. J.*, vol. 1, no. 2, pp. 41-59, Autumn 1996.
- [5] H. El Gamal, and A. R. Hammons, "On the design and performance of algebraic space-time codes for BPSK and QPSK modulation," *IEEE Trans. Commun.*, vol. 50, pp. 907-913, June 2002.
- [6] B. Hassibi and B. Hochwald, "High-rate codes that are linear in space and time," in *Proc. Allerton Conf. Commun., Cont. Comput.*, Oct. 2000.
- [7] K. Y. Wu, *Semi-Random Forward Error Correction Codes and Space-Time Codes*, Ph.D. Thesis, City University of Hong Kong. (www.ee.cityu.edu.hk/~liping).
- [8] S. ten Brink, "Convergence behavior of iteratively decoded parallel concatenated codes," *IEEE Trans. on Commun.*, vol. 49, pp. 1727-1737, Oct. 2001.
- [9] F. N. Brannstrom, T. M. Aulin, and L. K. Rasmussen, "Iterative decoders for trellis code multiple-access," *IEEE Trans. on Commun.*, vol. 50, pp. 1478-1485, Sept. 2002.
- [10] T. S. Rappaport, *Wireless Communications Principle and Practice*. Prentice-Hall. 1996.
- [11] T. M. Cover and J. A. Thomas, *Elements of Information Theory*. New York: Wiley, 1991.
- [12] I. M. Kim, and V. Tarokh, "Variable-rate space-time block codes in M -ary PSK systems," *IEEE Selected. Areas in Commun.*, vol. 21, pp. 362-373, Apr. 2003.
- [13] K. Y. Wu and Li Ping, "Multilayer turbo space-time codes", *IEEE Commun. Lett.* vol. 9, no. 1, pp. 55-57, Jan. 2005.
- [14] Li Ping, W. K. Leung, and K. Y. Wu, "Low-rate turbo-Hadamard codes," *IEEE Trans. Inform. Theory*, vol. 49, pp. 3213-3224, Dec. 2003.
- [15] Y. Gong and K. B. Letaief, "Concatenated space-time block coding with trellis coded modulation in fading channels," *IEEE Trans. Wireless Commun.*, vol. 4, pp. 580-590, Oct. 2002.
- [16] Z. Chen, B. S. Vucetic, J. Yuan, and K. L. Lo, "Space-time trellis codes for 4-PSK with three and four transmit antennas in quasi-static flat fading channels," *IEEE Commun. Lett.*, vol. 6, pp. 67-69, Feb. 2002.
- [17] J. N. Laneman, G. W. Wornell, "Distributed space-time-coded protocols for exploiting cooperative diversity in wireless networks," *IEEE Trans. on Inform. Theory*, vol. 49, pp. 2415-2424, Oct. 2003.